

© Copyright 2019

Wenqing Ju

Multiplexed Carbon Nanotube Sensing film for Smart Soil Application

Wenqing Ju

A thesis

submitted in partial fulfillment of the
requirements for the degree of

Master of Science in Mechanical Engineering

University of Washington

2019

Committee:

Jae-hyun Chung, Chair

Igor Novoselov

Sawyer Fuller

Program Authorized to Offer Degree:

Mechanical Engineering

University of Washington

Abstract

Multiplexed Carbon Nanotube Sensing film for Smart Soil Application

Wenqing Ju

Chair of the Supervisory Committee:
Associate Professor, Jae-Hyun Chung
Department of Mechanical Engineering

For smart management of soil, continuous monitoring of nitrogen (N) is essential. Current monitoring systems are either expensive or insensitive to nitrogen. The objective of this thesis is to develop an array of single walled carbon nanotube (SWCNT) sensors in order to monitor ammonia and NO_x diffused from the soil in a crop field. The array includes a pure SWCNT sensor, a nafion-coated SWCNT sensor and a polyethylenimine-coated SWCNT sensor. Using ammonia gas, the sensitivity and specificity of a SWCNT sensors are characterized. The calibrated sensors are tested for sand mixed with fertilizer in order to measure the concentration of ammonia and NO_x . The detection limit is evaluated in terms of the weight ratio of sand to fertilizer. The developed sensor with light weight and a small form factor can be embedded in an unmanned vehicle for smart management of soil and other environment.

TABLE OF CONTENTS

List of Figures	iii
List of Tables	v
Chapter 1. Introduction	1
1.1 Agriculture and nitrogen	1
1.2 The effect of ammonia on environment.....	3
1.3 Some common ammonia measurement methods.....	3
1.3.1. Gas chromatography	3
1.3.2. Mass spectrometry	5
1.3.3. Spectroscopy	6
1.3.4. Metal oxide semiconductor sensors	7
1.3.5. Detection tubes.....	7
1.3.6. Carbon nanotube sensors	7
1.3.7. Summary	9
Chapter 2. Methodology	10
2.1 Experiment design	10
2.2 Preparation of SWCNT sensors	11
2.3 MQ-135 calibration.....	12
2.4 SWCNT sensors' ammonia test	14
2.5 In-chamber Soil test	14
Chapter 3. Results and Discussion.....	16

3.1	MQ-135 calibration result and discussion	16
3.2	SWCNT sensors ammonia test result and discussion	16
2.2.1.	1ppm to 50ppm test results	16
2.2.2.	10ppb to 1ppm test results	19
2.2.3.	SWCNT sensors ammonia test discussion.....	21
3.3	SWCNT sensors soil test result and discussion	21
3.4	SWCNT sensors soil-sand mixture test result and discussion	23
3.5	Summery	29
	References.....	31
	Appendix A.....	34
	Appendix B.....	35

LIST OF FIGURES

Figure 1: Illustrations of gas chromatography. (a) principle of gas chromatography. (Pandey, 2013) (b) equipment set of gas chromatography. (Retrieved from <http://mytutorial.srtcube.com/gas-chromatography-gc/environment-science/826-520#7899>) (c) Chromatogram of the extract of an Armagnac by ether hexane (concentration about 3 times); column FFAP 50 m × 0.22 mm; injection according to splitless mode; temperature programming from 40 to 200°C. identification of the peaks: 1, Ethylbutyrate; 2, 2-methylpropan-1-ol; 3, isoamyl acetate; 4, isoamyl alcohols; 5, ethyl hexanoate; 6, hexyl acetate; 7, styrene; 8, acetoin; 9, ethyl heptanoate; 10, ethyl lactate; 11, hexan-1-ol; 12, trans-hex-3-en-1-ol; 13, cis-hex-3-en-1-ol; 14, octan-3-ol (internal standard 1); 15, trans-hex-2-en-1-ol; 16, ethyl octanoate; 17, trans-linalol oxide (furan); 18, cis-linalol oxide (furan), 19, acetic acid; 20, benzaldehyde; 21, linalol; 22, 2-methylpropionic acid; 23, ethyl decanoate; 24, butyric acid; 25, 3-methylbutyric acid; 26, diethyl succinate; 27, α-terpineol; 28, 1,1,6-trimethyl-1,2-dihydronaphthalene (TDN); 29, methionol; 30, inconnu; 31, inconnu; 32, damascenone; 33, phenylethyl acetate; 34, ethyl dodecanoate + hexanoic acid; 35, benzyl alcohol; 36, trans-whisky lactone; 37, 2-phenylethanol; 38; cis-whisky lactone; 39, 4-ethylgaiacol; 40, ethyl myristate; 41, octanoic acid; 42, 4-allylgaiacol (eugenol); 43, 4-ethylphenol; 44, ethyl palmitate; 45, decanoic acid; 46, ethyl stearate; 47, ethyl oleate; 48, dodecanoic acid; 49, ethyl linoleate; 50, ethyl linolenate; 51, inconnu; 52, myristic acid; 53, palmitic acid; 54, palmitoleic; 55, linoleic acid. Adapted from [22]...... 4

Figure 2: Sketch of the Non Dispersive Infra-Red (NDIR) carbon dioxide (CO₂) sensor structure. Adapted from [26]..... 6

Figure 3: Three types of SWCNT sensors. Left: pure SWCNT sensor. Middle: Nafion-coated SWCNT sensor. Right: PEI-coated SWCNT sensor. 12

Figure 4: (a) The typical sensitivity characteristics of the MQ-135 for several gases (20 °C, 65% humidity, 21% O₂ concentration). (b) the typical dependence of the MQ-135 on temperature and humidity. 13

Figure 5: Drone set up for the drone test. Left: front view. Right: the 3D printed case for the battery and the Arduino board. 15

Figure 6: Calibration curve for MQ-135 ammonia sensor 16

Figure 7: 1ppm to 50ppm test results (a) calibration curve for pure SWCNT sensors resistance changes at 650 seconds. (b) Calibration curve for Nafion-coated SWCNT sensors resistance changes at 650 seconds. (c) PEI-coated SWCNT sensors resistance changes through the test. 18

Figure 8: 10ppb to 1ppm test results (a) calibration curve for pure SWCNT sensors resistance changes in 650 seconds. (b) Calibration curve for Nafion-coated SWCNT sensors resistance changes in 650 seconds. (c) PEI-coated SWCNT sensors resistance changes through the test 20

Figure 9: Fertilized soil test results. (a) Pure SWCNT sensors resistance changes. (b) Nafion-coated SWCNT sensors resistance changes. (c) PEI-coated SWCNT sensors resistance changes..... 23

Figure 10: Soil-sand mixture test results. (a) Pure SWCNT sensors resistance (b) Nafion-coated SWCNT sensors resistance changes (c) PEI-coated SWCNT sensors resistance changes. All the tests started at 150s and ended at 800s..... 25

Figure 11: soil-sand mixture in the Pyrex® 150x75 mm crystallizing dish. 25

Figure 12: Drone test result. (a) Drone test timeline. (b) Pure SWCNT resistance change. (c) Nafion-coated SWCNT resistance change. (d) PEI-coated SWCNT resistance change. 28

LIST OF TABLES

Table 1.1. Comparison of ammonia sensing methods	9
--	---

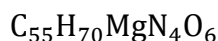
ACKNOWLEDGEMENTS

I would like to give my special appreciation to my supervisor, Prof Chung, for all the valuable guidance and great encouragement he gave me. Also, thanks to my thesis committee for all the supports from them. Besides, thanks to my beloved family and my girlfriend, for accompanying me when I worked late or worked on weekends.

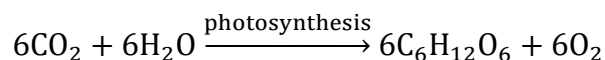
Chapter 1. INTRODUCTION

1.1 AGRICULTURE AND NITROGEN

The effect of nitrogen on plants, especially crops, is widely studied. Nitrogen (N) is an essential element for plants and has multiple forms in plants. Nucleic acids, genetic material, have nitrogenous base that contains nitrogen. Proteins, which can be found in plant structures, must have CO-NH bonds in the molecular formula. Chlorophyll, the essential molecule for photosynthesis, consists of N element. For example, chlorophyll b, a form of chlorophyll, has the following molecular formula:



in which there are four nitrogen atoms. Through photosynthesis, plants use solar energy to produce carbohydrate and oxygen from water and carbon dioxide:

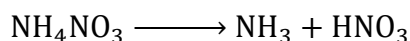


When nitrogen deficiency happens, the growth rate of the plants slows down. Then the plants have a trend to be slender and have abnormal branching [1, 2]. Except for chlorophyll, green leaves also have carotene and xanthophyll, yellow color pigments. Normally, these pigments are covered with chlorophyll. Since the plants are unable to absorb enough nitrogen to generate sufficient chlorophyll, their leaves appear pale green or yellow in color. Such symptom is known as firing.

Even though nitrogen is crucial for plants, it is deficient in terrestrial ecosystems. Nitrogen gas (N_2) occupies about 80% of atmosphere [2], but it is a form that cannot be absorbed by plants directly. Plants absorb inorganic nitrogen compounds (*i.e.*, NH_4^+ , NO_2^- , and NO_3^-) from soil [3]. Thus, the supply of nitrogen increases the yield and has become a fundamental feature of modern crop management [4]. In agriculture, fertilizers are widely used as the main sources of additional

nitrogen. The effect of that additional nitrogen can be significant. When sunflowers (*Helianthus annuus* L. var. CATISSOL-01) were provide with large amount of ammonium nitrate solution (282 ppm of nitrogen), the shoot dry matter of the plants were almost four-fold compared with the sunflowers that were provided with small amount of ammonium nitrate solution (28.2 ppm of nitrogen) [5]. Corns (*Zea mays* L. cv. 33A14) with 20% N treatment had about 20% more shoot biomass accumulated than the corns with 0% N treatment after 42 days after emergence [6].

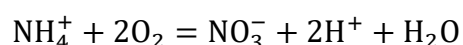
Although additional nitrogen promotes economic performance, overuse or misuse of those nitrogen sources will cause the loss of nitrogen. Many fertilizer companies use ammonium nitrate (NH_4NO_3) in the fertilizer as nitrogen source and ammonium nitrate can decompose to generate ammonia [7].



This means that overuse of fertilizers not only reduce the cost efficiency, but also generate extra nitrogen that will enter water body or atmosphere as ammonia and oxides of nitrogen like nitrous oxide [8]. Some research has proved that those nitrogen compounds could have a negative effect on the environment [9, 10]. In fact, agricultural activities contribute 80%-90% of the ammonia in atmosphere, and synthetic fertilizers is one of the main sources of the contribution [11]. Some other minor ammonia sources are human breath, industry, mobile sources, publicly owned treatment works, wild animals, forest fires, slash burning and domestic animals [7]. As a result, in agriculture, people very early began to detect the nitrogen level in the soil and atmosphere to help reasonable use of manure and fertilizers.

1.2 THE EFFECT OF AMMONIA ON ENVIRONMENT

Until 2004, emissions of nitrogen to the atmosphere have increased about five times compare with pre-industrial times [12, 13], and one of reasons is the use of fertilizer [4]. Researchers have found that the excess nitrogen is a threat to European terrestrial biodiversity, and particularly, gaseous ammonia can damage to vegetation [14]. Also, not only in Europe, in North America and Asia, severe nitrogen deposition is influencing the forest productivity by eutrophication and acidification. In areas where there is sufficient N, the nitrophilic species can grow relatively faster, and thus capture the living spaces for other species. Also affected by the ammonium-based fertilizers, the soil's pH can be largely decrease through nitrification [15]:



Nitrite (NO_3^-) is the form of nitrogen that can be absorbed by crops, but when there are too much of the fertilizers, the excess nitrite will acidify the soil. Only the species that are able to sustain low pH can live in such soil. Plus, the low pH reduces environment's ability to decompose organic material, which leads to litter accumulation. [10, 16-18]. Even though in Europe, the emission rate of ammonia has decreased in the past three decades [19], there is still a large amount of ammonia remain, which increase the recovery time of the forest ecosystem. According to a prediction form Galloway et al. [12, 20], in 2050, global nitrogen will reach 200 Tg N year⁻¹.

1.3 SOME COMMON AMMONIA MEASUREMENT METHODS

1.3.1 Gas chromatography

Gas chromatography (GC) is greatly used in laboratory research for segregating and analyzing compounds that can be vaporized without decomposition [21]. Figure 1 (a) shows the principle of GC, and Figure 1 (b) shows the GC experiment set. Gas chromatography uses inert

gas (mostly is helium) as carrier gas. The carrier gas carries the gaseous compounds through a column which is coated with a layer of liquid or polymer (called stationary phase). Different compounds have a different interaction with the column. When the affinity of the compound is less for the stationary phase, only a small portion of the compound will be captured by the column, and thus it will be eluted and detected first. For those compounds that have more affinity to the stationary phase will retain in the column for a longer time. Figure 1(c) is a GC result for components contained in a nether-hexane extract of Very Special Old Pale Armagnac [22]. The x-axis is time and the peaks at different times mean there were different compounds detected over time. This type of method has a good resolution, high repeatability, high precision but also high cost.

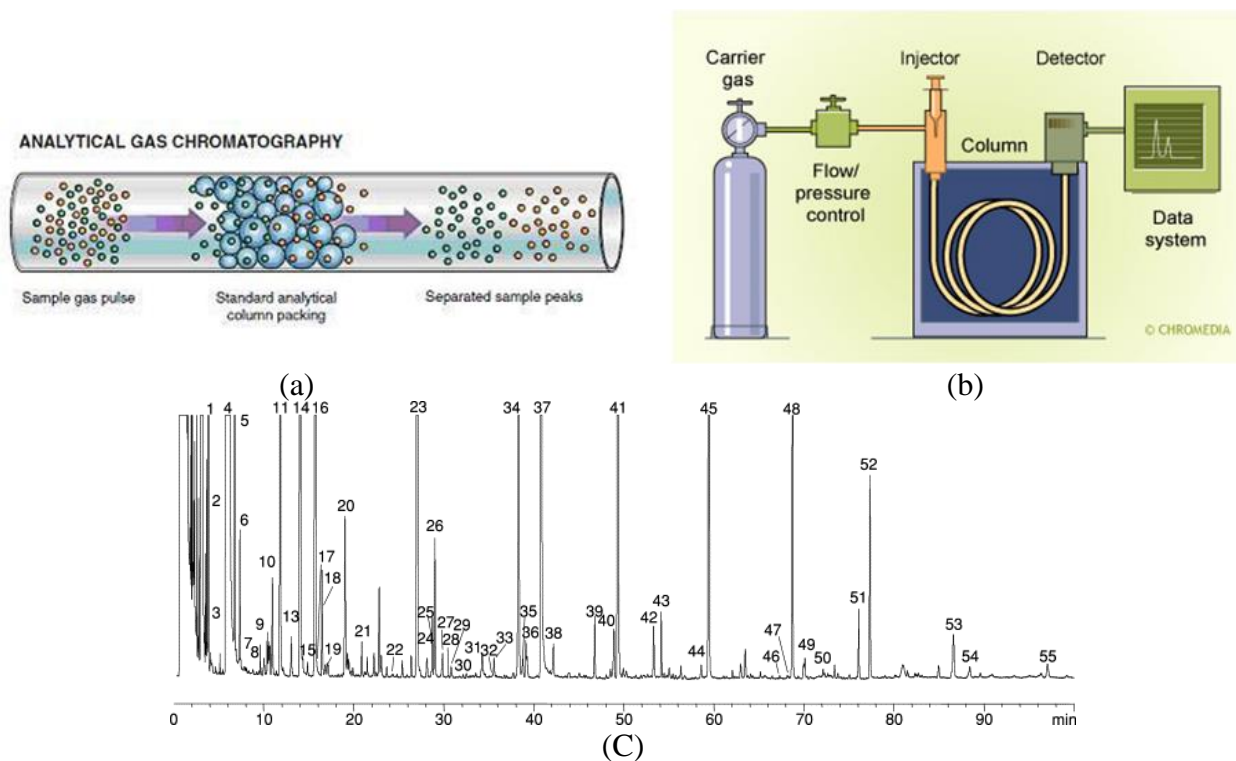


Figure 1: Illustrations of gas chromatography. (a) principle of gas chromatography. (Pandey, 2013) (b) equipment set of gas chromatography. (Retrieved from <http://mytutorial.srtcube.com/gas-chromatography-gc/environment-science/826-520#7899>) (c)

Chromatogram of the extract of an Armagnac by ether hexane (concentration about 3 times); column FFAP 50 m × 0.22 mm; injection according to splitless mode; temperature programming from 40 to 200°C. identification of the peaks: 1, Ethylbutyrate; 2, 2-methylpropan-1-ol; 3, isoamyl acetate; 4, isoamyl alcohols; 5, ethyl hexanoate; 6, hexyl acetate; 7, styrene; 8, acetoin; 9, ethyl heptanoate; 10, ethyl lactate; 11, hexan-1-ol; 12, trans-hex-3-en-1-ol; 13, cis-hex-3-en-1-ol; 14, octan-3-ol (internal standard 1); 15, trans-hex-2-en-1-ol; 16, ethyl octanoate; 17, trans-linalol oxide (furan); 18, cis-linalol oxide (furan), 19, acetic acid; 20, benzaldehyde; 21, linalol; 22, 2-methylpropionic acid; 23, ethyl decanoate; 24, butyric acid; 25, 3-methylbutyric acid; 26, diethyl succinate; 27, α -terpineol; 28, 1,1,6-trimethyl-1,2-dihydronaphthalene (TDN); 29, methionol; 30, inconnu; 31, inconnu; 32, damascenone; 33, phenylethyl acetate; 34, ethyl dodecanoate + hexanoic acid; 35, benzyl alcohol; 36, trans-whisky lactone; 37, 2-phenylethanol; 38; cis-whisky lactone; 39, 4-ethylgaiacol; 40, ethyl myristate; 41, octanoic acid; 42, 4-allylgaiacol (eugenol); 43, 4-ethylphenol; 44, ethyl palmitate; 45, decanoic acid; 46, ethyl stearate; 47, ethyl oleate; 48, dodecanoic acid; 49, ethyl linoleate; 50, ethyl linolenate; 51, inconnu; 52, myristic acid; 53, palmitic acid; 54, palmitoleic; 55, linoleic acid.

Adapted from [22].

1.3.2 Mass spectrometry

The mass spectrometer ionizes the sample and separates the ions. The separation is achieved by accelerating the ions and applying an electric or magnetic field, so that the ions with different mass-to-charge ratio will have different deflection angles [23]. Later, the separated ions are detected, and are shown as a spectrum with an order on the basis of the ions' mass-to-charge ratio. The sample is not limited to gas but could also be solid or liquid. Mass spectrometry has a very high sensitivity that can reach sub-ppb level [24]. The instrument costs can be from a few

thousands to over a hundred thousand US dollars, and operation costs vary from analytes of mass spectrometry. Mass spectrometry sometimes is combined with gas chromatography to more accurately analyze the compound.

1.3.3 Spectroscopy

Spectroscopy's working mechanism is based on absorption and emission spectrometry. Every gas at different wavelengths has different absorbing rate. A typical and widely used spectroscopy sensor is infrared (IR) gas sensor. It contains IR source, gas chamber and IR detector. The IR source emits the radiation and the target gas absorbs a certain wavelength. Then the detector can screen the wavelength except for the absorbed wavelength. An illustration of IR gas detecting system is shown in Figure 2. This type of sensor is mostly used for gas leak detection and air quality monitoring. For example, the Infrared Atmospheric Sounding Interferometer (IASI) was installed on a satellite and used for monitoring global ammonia distribution [25]. It measures infrared radiation in the spectral range $645\text{-}2760\text{ cm}^{-1}$, and ammonia absorbs the $750\text{-}1200\text{ cm}^{-1}$ range. The ammonia concentration can be calculated through some specific methods.

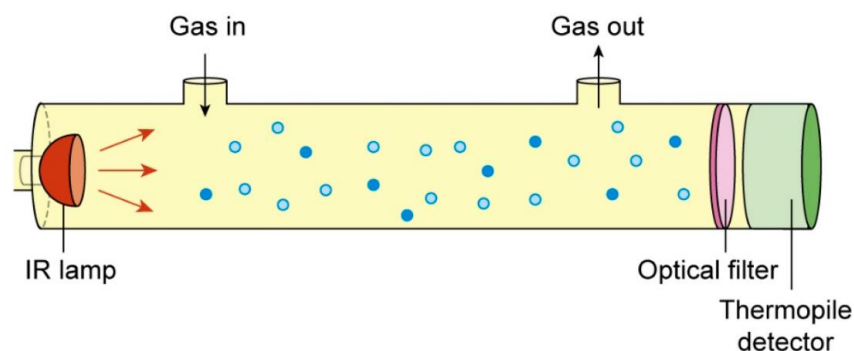


Figure 2: Sketch of the Non Dispersive Infra-Red (NDIR) carbon dioxide (CO₂) sensor structure. Adapted from [26].

1.3.4 Metal oxide semiconductor sensors

Metal oxide semiconductors are the most frequent sensing materials [27]. When the sensor is exposed to the monitored gas, the oxygen ion (O^-) on the surface of the semiconductor is reduced by the gas (like ammonia). This redox reaction causes the resistance decreasing of the sensor [27] [28]. Usually, a heat source is added to the sensor to increase its sensitivity.

Semiconductor sensors have a fast reaction time, the normal lower detection limit is about 1ppm, and the cost is low. Because of this sensing mechanism, the major disadvantage of metal oxide semiconductor sensors is that it can react with multiple types of gases, so the sensing target is not selective. The MQ135 ammonia sensor that is used in the experiment is a metal oxide semiconductor sensor.

1.3.5 Detection tubes

Detection tubes have a low cost, but the accuracy is low [29]. The measuring mechanism of detection tubes is the coated acid on the tube switch to different colors when reacts with different concentration of ammonia.

1.3.6 Carbon nanotube sensors

Carbon nanotubes (CNTs) are widely used on gas sensors, temperature/humidity sensors, stress/strain sensors and biosensors, etc. CNTs are either metallic or semiconducting and their chemical structure makes them have a large surface-area-to-volume ratio. Because of the unique properties, CNTs are highly sensitive to some low concentration gases (like alcohol or carbon dioxide) at room temperature. Moreover, the manufacturing process of CNT sensors eliminates the need of microfabrication, which is required for semiconductor sensors; the cost of CNT sensors is lower than semiconductor sensors. The response times of CNT sensors vary from different target

gases [30]. A disadvantage of CNT sensor is that it is not selective, which means the response of the sensor can be the contribution of multiple gases. To increase the specificity and sensitivity, polymers and/or metal nanoparticles are often added during the manufacturing process.

A lot of researchers have developed different types of ammonia sensors using carbon nanotubes. Han et al. [31] implemented single-walled carbon nanotubes (SWCNT) on cotton yarns and used gold (Au) as sensor's electrodes. The detection limit of their sensor was 8ppm. Goudarzi et al. [32] doped SWCNTs with lithium and dispersed on interdigitated electrodes using electrophoresis method. Then the sensors were heat treated at 350°C for 5 hours. This type of sensor has 29% of sensitivity to 500ppm ammonia at 25°C. Young et al. [33] used thermal chemical vapor deposition (CVD) method to grow high-density CNTs on oxidized Si substrates. They tested the sensor with ammonia concentration range from 50ppm to 800ppm. At 50ppm, their sensor had about 1% sensitivity and about 500 seconds of response time. Randeniya et al. [34] treated CNT yarns with strong acid or in a pulsed direct-current plasma and used self-fuelled electrodeposition method to aggregate Au nanoparticles onto CNT yarns. The lowest detectable ammonia concentration was around 500ppb, and plasma treated and Au decorated sensor samples were stable, reusable and able to recovery. Chiesa et al. [35] developed a low-cost sensing system. The ammonia sensor was made by drop casting SWCNT solution on plastic or ceramic substrates, and connected CNTs and Pt electrodes by Ag contacts. A humidity and temperature sensor was mounted to the system for calibration purpose. They also developed Expert System algorithms to help calculate the concentration. Their sensing system can response to about 10 ppb of ammonia with an error of 20%.

1.3.7 Summary

Table 1 list all the ammonia sensing methods discussed above and their advantages and disadvantages.

Table 1.1. Comparison of ammonia sensing methods

methods	Advantage	Disadvantage
Gas chromatography	High sensitivity and specificity	High cost and large in equipment size
Mass spectrometry	High sensitivity and specificity	High cost and large in equipment size
spectroscopy	High specificity	High cost and large in equipment size
Metal oxide semiconductor sensors	Low cost and quick response	Low sensitivity and specificity. Needs to be heated
Detection tubes	Low cost and short response time	Low accuracy
Carbon nanotube sensors	Low cost and short response time	Relatively low specificity

Chapter 2. METHODOLOGY

2.1 EXPERIMENT DESIGN

The experiment consisted of five sections. The first section was the calibration of MQ-135 commercial ammonia sensor. MQ-135 was a semiconductor sensor with a detecting concentration scope from 10ppm to 300ppm. It was used as a reference sensor when the CNT sensors were tested in the range from 10ppm to 100ppm.

The second section of the experiment was the preparation of CNT sensors. Three types of CNT sensors were selected for this experiment. The first type was a pure CNT sensor without any coating. The second type and the third type were a CNT sensor coated with Nafion and polyethylenimine (PEI), respectively. In type 2 and type 3, CNT sensors coated with different concentrations of Nafion and PEI were also made for studying the concentration for a higher sensitivity (i.e. the sensor will have the best sensitivity). The reason for preparing three different types of sensors was that CNT sensors could not selectively target one specific gas. To enhance the specificity, the sensors with different polymers and concentrations were selected. Pure CNT sensors and Nafion-coated CNT sensors were expected to be p-type [36]. When exposed to ammonia, the resistance of the sensors increased. The PEI-coated SWCNT sensors were expected to be n-type and had a decrease in resistance when exposed to ammonia [37]. In a field test stage, all types of the sensors were used for detecting ammonia.

The third section of the experiment was to test the CNT sensors in a chamber with different concentrations of ammonia, from 10ppb to 100ppm. The purpose of the chamber test was to find the best concentration of Nafion and PEI for coating and to characterize the sensor response. The ppm level test (from 10ppm to 100ppm) was conducted first. The use of MQ-135

in this concentration level guaranteed the accuracy when plotted the sensitivity characteristic curve for SWCNT sensors. Subsequently, the ppb level test (from 10ppb to 10ppm) was conducted.

The fourth part was in-chamber soil test. The SWCNT sensors were tested with different amount of fertilized soils. Later these soils were mixed with 1kg of non-fertilized sand to evaluate the minimum soil-sand ratio that the SWCNT sensors could detect.

The fifth part of the experiment was a drone test. The SWCNT sensors were installed to a drone. The drone flied to soil that emitted ammonia. By analyzing the different response of the sensors and comparing the results with chamber test, an estimation of the ammonia concentration could be given.

The whole experiment used an Arduino Uno board to drive the MQ-135 sensor and SWCNT sensors. A H&T sensor were added for calibrating the ammonia sensors from humidity and temperature effect. The data was transported through a Bluetooth kit. The circuit design is described in Appendix A. The Arduino code could be found in Appendix B.

2.2 PREPARATION OF SWCNT SENSORS

Three types of SWCNT sensors were prepared. Single walled carbon nanotubes (SWCNTs) were dispersed in SDS at a concentration of 1mg/mL using a sonicator at room temperature for 8 hours. The SWCNTs were spin-coated on a PET film at 6000 rpm for 1 minute. Silver ink was stamped on the SWCNT surface. The first type of SWCNT sensors were used without any additional coating layers. The second type of the SWCNT sensors were coated with two different concentrations of Nafion: 0.1% and 0.5%. The Nafion was spin coated for 10 seconds and heat treated on 120 °C hot plate for 10 minutes. The third type of the SWCNT sensors were coated with two different concentrations of PEI: 0.1% and 0.5%. The PEI was doped on the sensors and

heat treated on 100 °C hot plate for 10 minutes. The electrodes and the electric wires were connected by silver paste. Figure 3 shows those 3 different types of sensors. The white parts were the silver electrodes. This type of design can largely increase the interacting area between the SWCNTs and target gases.

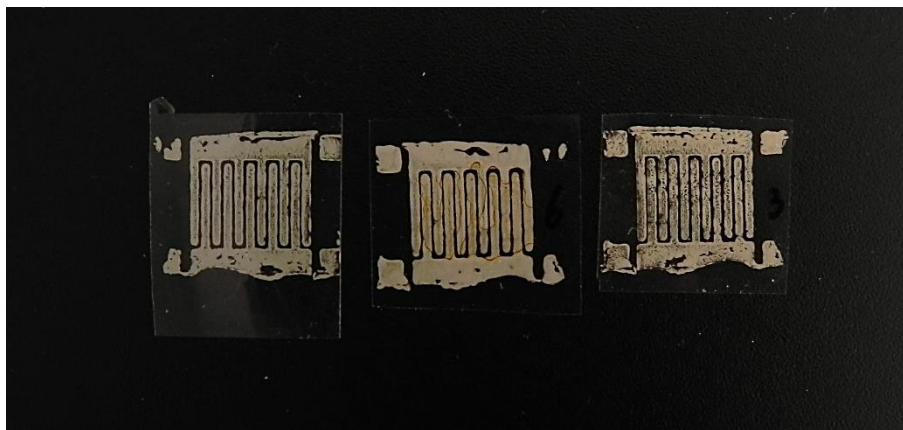
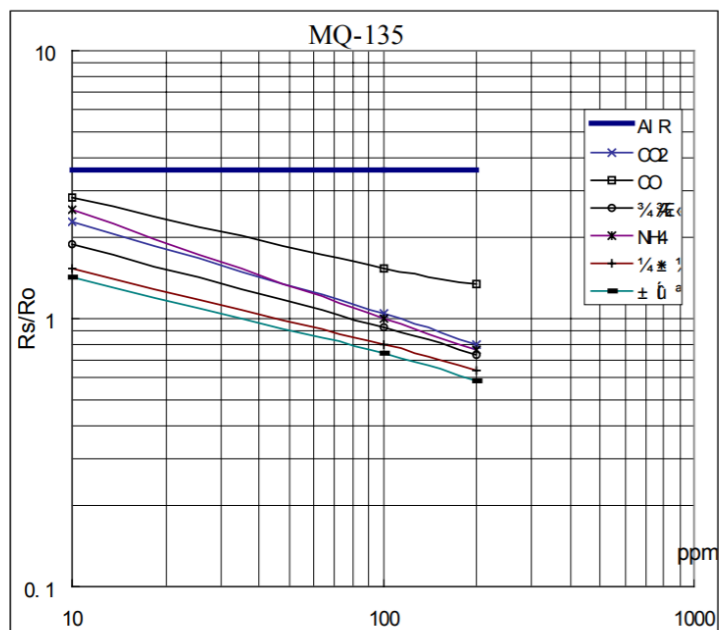


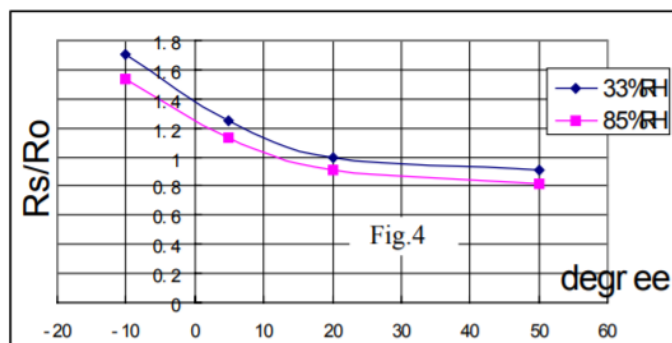
Figure 3: Three types of SWCNT sensors. Left: pure SWCNT sensor. Middle: Nafion-coated SWCNT sensor. Right: PEI-coated SWCNT sensor.

2.3 MQ-135 CALIBRATION

A MQ-135 sensor was calibrated as the manufacturer's recommendation. There were two important parameters of the sensor. One is R_0 , which is the sensor resistance at 100 ppm of ammonia in the clean air. The other is R_s , which is the sensor resistance at various concentration of gases. Figure 4(a) shows the calibration curves by the manufacturer. The R_s/R_0 ratio changes are compared with ammonia concentration. A similar curve was expected after the calibration.



(a)



(b)

Figure 4: (a) The typical sensitivity characteristics of the MQ-135 for several gases (20 °C, 65% humidity, 21% O₂ concentration). (b) the typical dependence of the MQ-135 on temperature and humidity.

Before the calibration, the MQ-135 was pre-heated over 24 hours to reach the best working condition. MQ-135 was supposed to be placed into a closed chamber and exposed to 100 ppm of ammonia until the reading was stable. This step was to find R_0 . Limited by the lab condition, the MQ-135 was only tested under the concentration of 10ppm, 20ppm and 50ppm to determine the sensitivity characteristic curve. The test readings were already calibrated from humidity and temperature effect in the Arduino code.

2.4 SWCNT SENSORS' AMMONIA TEST

The SWCNT sensors' ammonia test was done by two parts. The first part was ppm level test (1ppm to 50ppm) with MQ-135 as a reference. The test was done under the concentration of 1ppm, 10ppm, 20ppm and 50ppm in a closed chamber for 650 seconds. (No ammonia from 0-150 seconds. Ammonia source applied from 150-800 seconds. Ammonia source was removed after 800 seconds. For rest of the experiment, all the ammonia source, fertilized soil sample, and soil-sand mixture were applied for 150~800 seconds) The second part was ppb level test (10ppb to 1ppm). In this range the MQ-135 was not accurate anymore. The test was conducted under the concentrations of 10ppb, 50ppb and 100ppb in a closed chamber for 650 seconds. Before each test, the SWCNT sensors' resistances were waited until they were fully recovered.

2.5 IN-CHAMBER SOIL TEST

The first part of the soil test was to test SWCNT sensors with 0.1g, 0.5g, 1g, 5g, 10g, and 30g fertilized soil sample contained in a Pyrex® crystallizing dish (150 x 75 No. 3140). The SWCNT sensors were tested in a sealed chamber with soil placed. The 0g test was conducted first as a control group to eliminate the effect from the residual in the chamber that might affect the test

results. For each test, the soils were placed in the chamber for 650 seconds and removed afterwards.

The second part of the soil test was to mix 0g, 0.1g, 0.5g, 1g, 5g, 10g, and 30g fertilized soil with 1kg of sand which did not have any fertilizer. The mixture was contained in a Pyrex[®] crystallizing dish (150 x 75 No. 3140). The test that with 0g of soil was conducted first as a control group. For each test, the soil-sand mixtures were placed in the chamber for 650 seconds and removed afterwards.

2.6 DRONE TEST

An Arduino board with SWCNT sensors, a Bluetooth module and a battery pack were put in a 3D-printed case and attached to a Dji Phantom 2 drone (shown in figure 5). The drone flew to a pot of fertilized soil (150g) and wait for 650 seconds. The test was done in the lab.



Figure 5: Drone set up for the drone test. Left: front view. Right: the 3D printed case for the battery and the Arduino board.

Chapter 3. RESULTS AND DISCUSSION

3.1 MQ-135 CALIBRATION RESULT AND DISCUSSION

The MQ-135 was calibrated and the calibration curve is shown in figure 5. The environment of 10ppm, 20ppm and 50ppm of ammonia was created for the calibration. The value of R_0 was 781 Ohms. The result shows a power relationship. This characteristic curve would be used as a reference when the SWCNT ammonia sensors were tested.

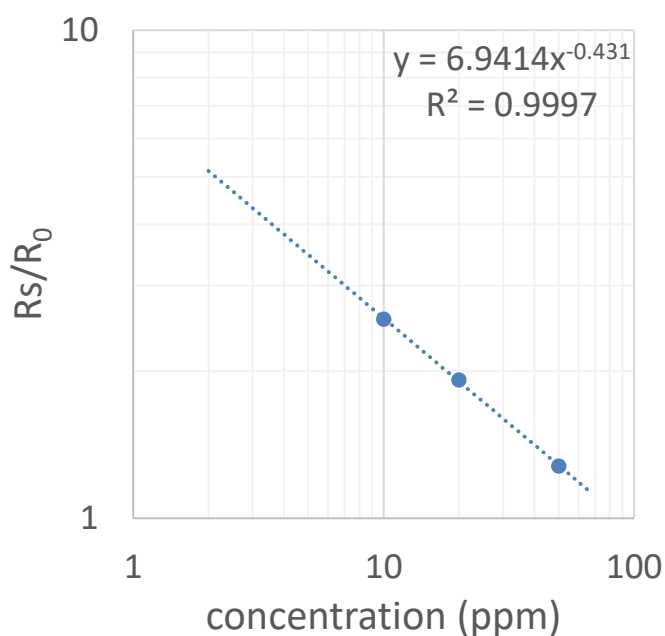


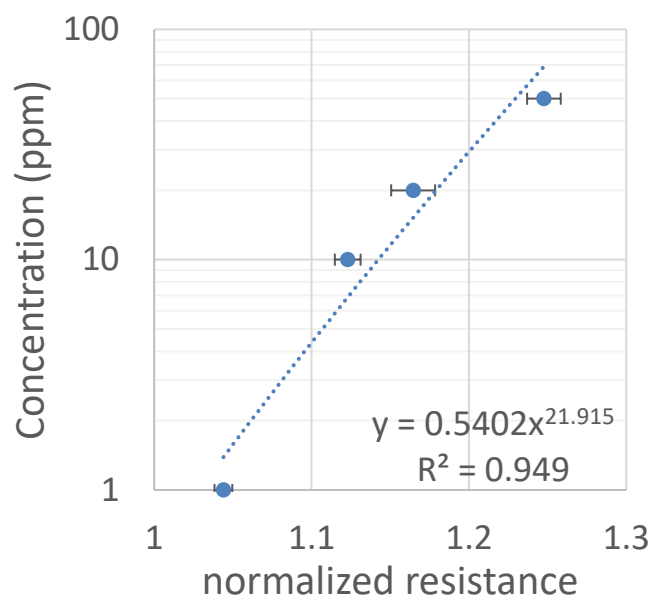
Figure 6: Calibration curve for MQ-135 ammonia sensor

3.2 SWCNT SENSORS AMMONIA TEST RESULT AND DISCUSSION

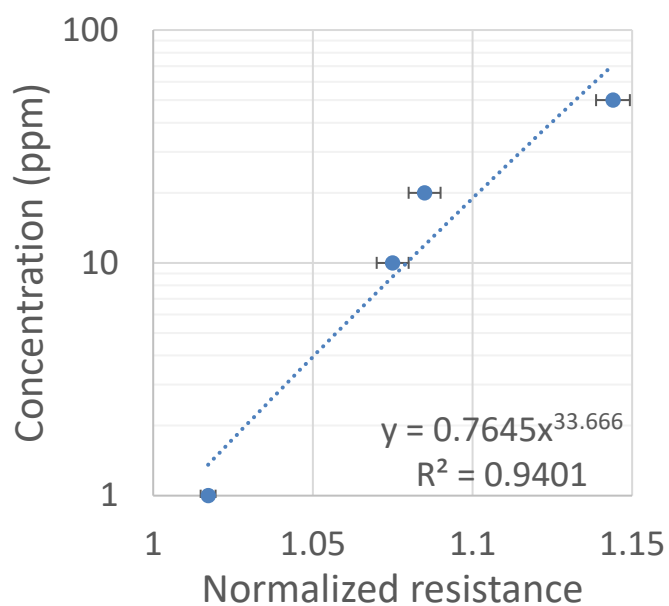
3.2.1 1ppm to 50ppm test results

The test result showed that the 0.1% Nafion-coated SWCNT sensors and the 0.1% PEI-coated SWCNT sensors performed better than 0.5% Nafion-coated SWCNT sensors and the 0.5% PEI-

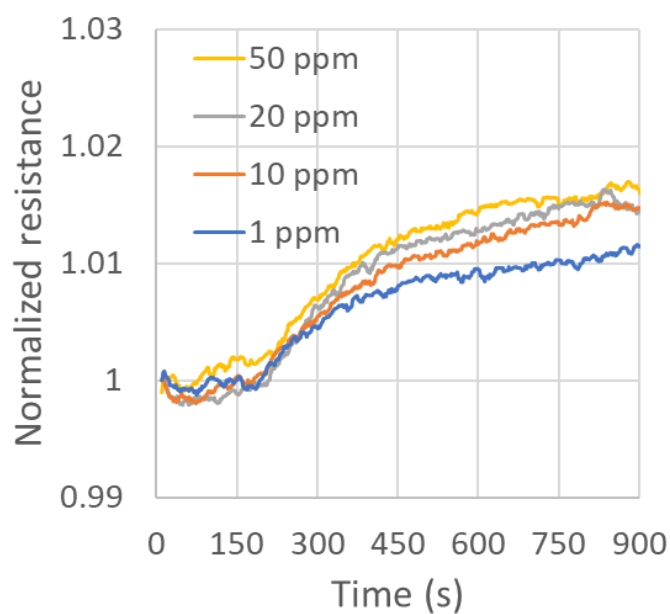
coated SWCNT sensors, respectively. The rest of the experiment used 0.1% Nafion-coated SWCNT sensors and the 0.1% PEI-coated SWCNT sensors. Figure 6 (a) and (b) gives the resistance changes of the pure SWCNT sensors and Nafion-coated SWCNT sensors at 800 seconds of the test. Figure 6 (c) shows the resistance change of a PEI-coated SWCNT sensor through the test. All types of sensors showed an increase of resistance in the test. Among them, the pure SWCNT sensors had the largest resistance change. Nafion-coated SWCNT sensors had a slightly less change than pure SWCNT sensors. PEI-coated sensors had a minor response to ammonia in comparison to the other two types of sensors.



(a)



(b)



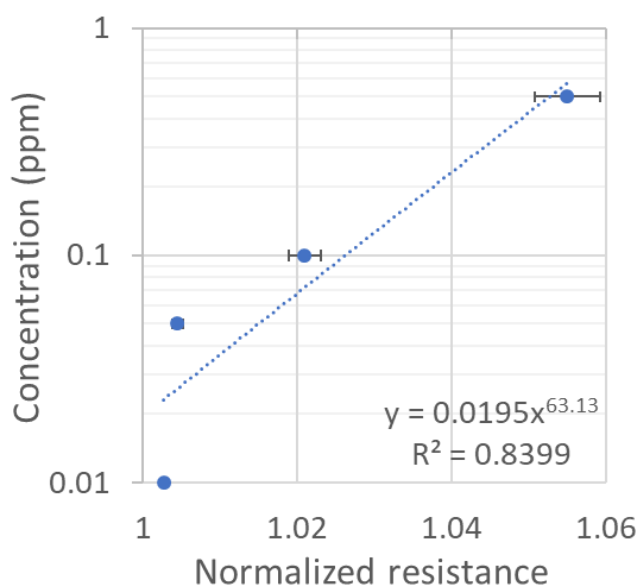
(c)

Figure 7: 1ppm to 50ppm test results (a) calibration curve for pure SWCNT sensors resistance changes at 650 seconds. (b) Calibration curve for Nafion-coated SWCNT sensors

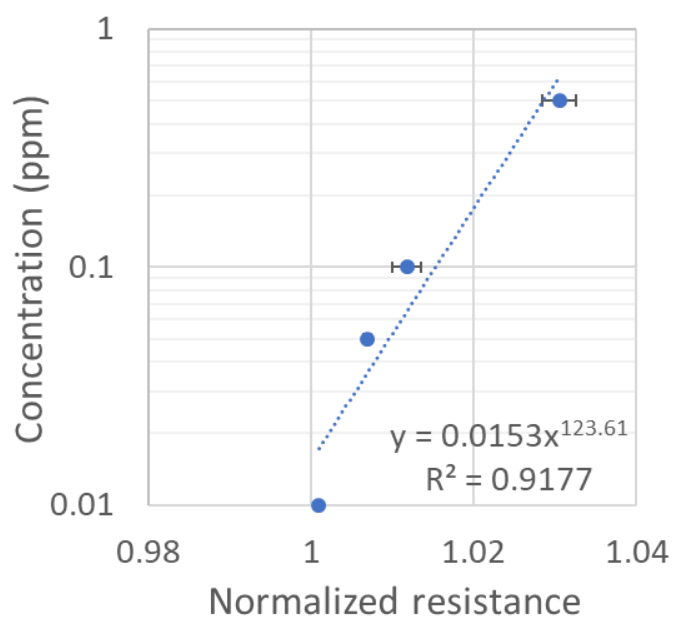
resistance changes at 650 seconds. (c) PEI-coated SWCNT sensors resistance changes through the test.

3.2.2 10ppb to 1ppm test results

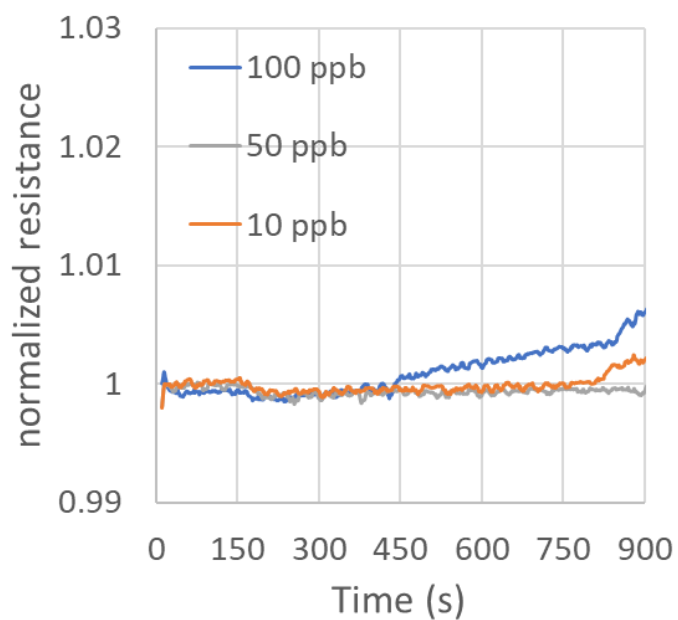
Figure 7 (a) and (b) gives the resistance changes of the pure SWCNT sensors and Nafion-coated SWCNT sensors at 800 seconds of the test. Both sensors showed a resistance increase yet the PEI-coated SWCNT sensors showed a minor resistance decrease. Figure 7 (c) shows the resistance change of a PEI-coated SWCNT sensor through the test.



(a)



(b)



(c)

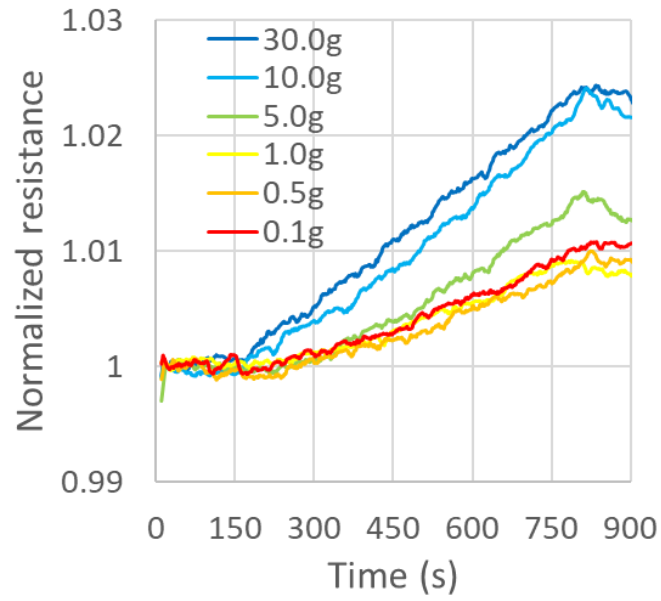
Figure 8: 10ppb to 1ppm test results (a) calibration curve for pure SWCNT sensors resistance changes in 650 seconds. (b) Calibration curve for Nafion-coated SWCNT sensors resistance changes in 650 seconds. (c) PEI-coated SWCNT sensors resistance changes through the test

3.2.3 SWCNT sensors ammonia test discussion

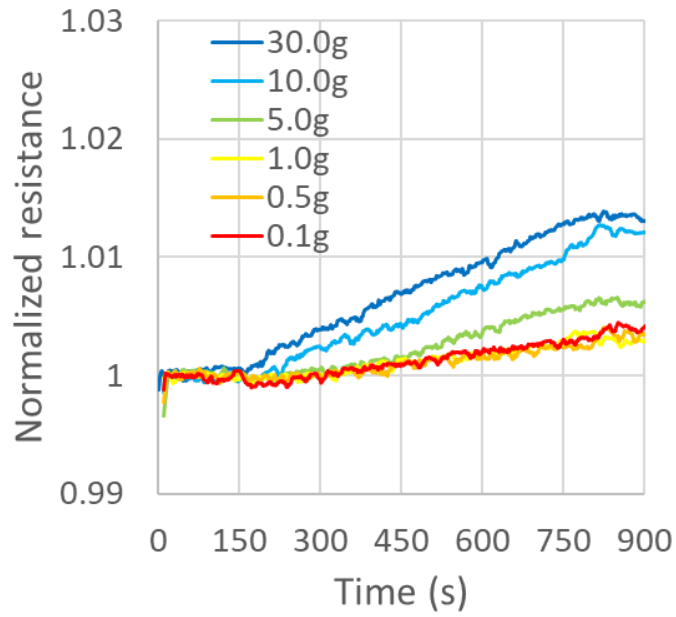
Compared with a ppb level test, the ppm level test had a more quantitative characteristic for the pure SWCNT sensors and the Nafion-coated sensors. Even though the PEI-coated SWCNT sensors had a minor resistance change, the resistance increased when the ammonia concentration was at ppm level. The resistance decreased when the ammonia concentration was at ppb level. Especially for the 100ppb test, the resistance decreased first and later increased. It was speculated that PEI-coated SWCNT sensors were n-type, but with the effect of high concentration of ammonia, those sensors might switch to p-type.

3.3 SWCNT SENSORS SOIL TEST RESULT AND DISCUSSION

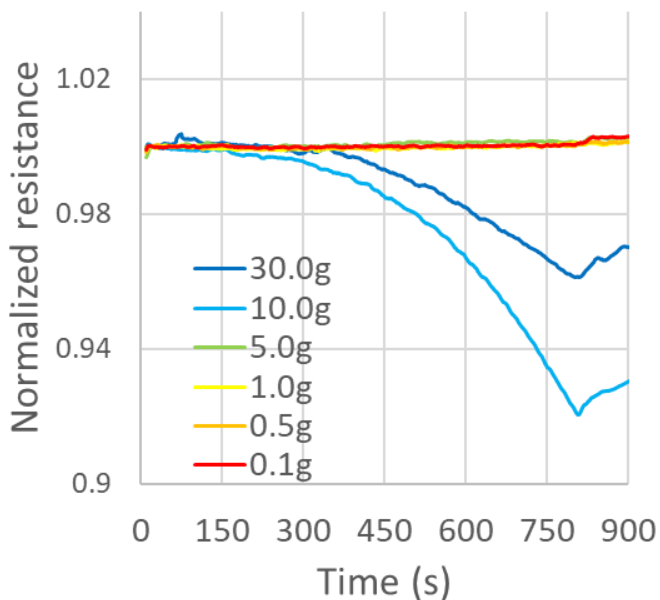
Figure 8 shows the SWCNT sensors soil test result. When tested with 0.1g, 0.5g and 1g of fertilized soil, there were no significant difference in the resistance change for all type of SWCNT sensors. As the soil amount increased to 5g, significant difference appeared for pure SWCNT sensors and Nafion-coated sensors. For the 10g and 30g test, the PEI-coated sensor showed a significant decrease. Such difference did not even show in the ammonia test. Since fertilizer could react with oxygen and generate NO_x , it was speculated that PEI-coated sensors were not only sensitive to ammonia but also sensitive to NO_x gases. For the 30g soil test, the pure SWCNT sensor had a resistance change of 1.023 at 800 seconds, while the Nafion-coated SWCNT sensor had a resistance change of 1.014 at 800 seconds. According to the characteristic curves in figure 7(a) and figure 7(b), the ammonia concentration was around 90 ppb. As for the resistance decrease of the PEI-coated SWCNT sensors, other gases had a major contribution while ammonia had a minor contribution. In conclusion, the ammonia emitted from this 30g soil sample was estimated as 90ppb at maximum.



(a)



(b)

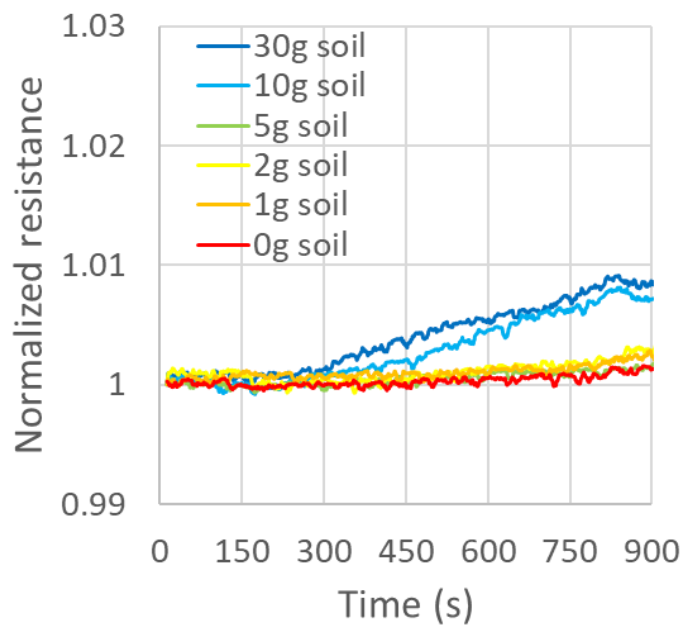


(c)

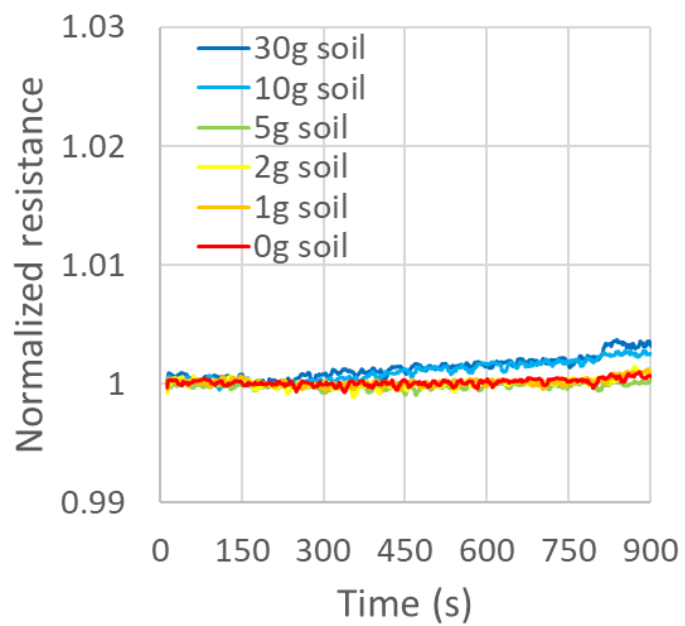
Figure 9: Fertilized soil test results. (a) Pure SWCNT sensors resistance changes. (b) Nafion-coated SWCNT sensors resistance changes. (c) PEI-coated SWCNT sensors resistance changes.

3.4 SWCNT SENSORS SOIL-SAND MIXTURE TEST RESULT AND DISCUSSION

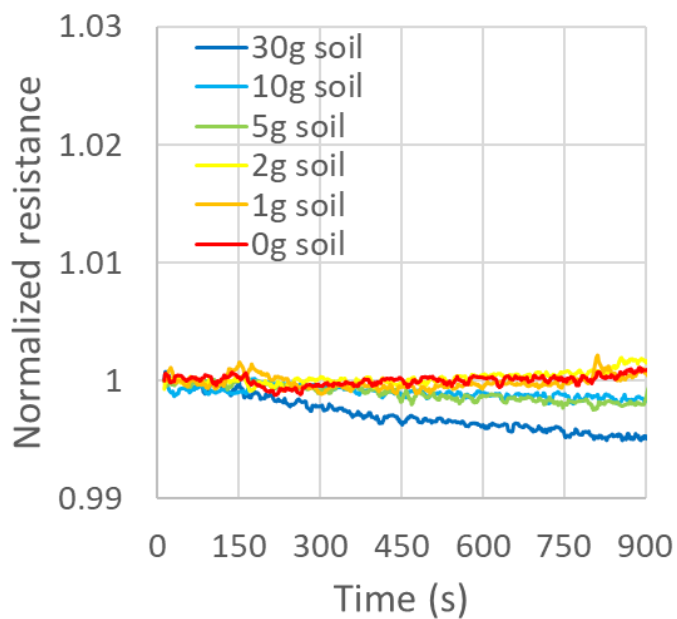
The soil-sand mixture test result is shown in figure 9. The significant difference in resistance change appeared after the 10g of soil mixed with the 1kg sand for the pure SWCNT sensor and the Nafion-coated sensor. As for the PEI-coated sensor, the decrease for 30g mixture test might be contributed by ammonia and NO_x gases. Even though there was a decrease for 30g mixture test, the decrease was much smaller than that from the 30g soil test. It was speculated that the sand in the mixture (the mixture is shown in figure 10) blocked some of the gas diffusion from the soil (ammonia and NO_x). The depth of the mixture was 3.7 cm.



(a)



(b)



(c)

Figure 10: Soil-sand mixture test results. (a) Pure SWCNT sensors resistance (b) Nafion-coated SWCNT sensors resistance changes (c) PEI-coated SWCNT sensors resistance changes.

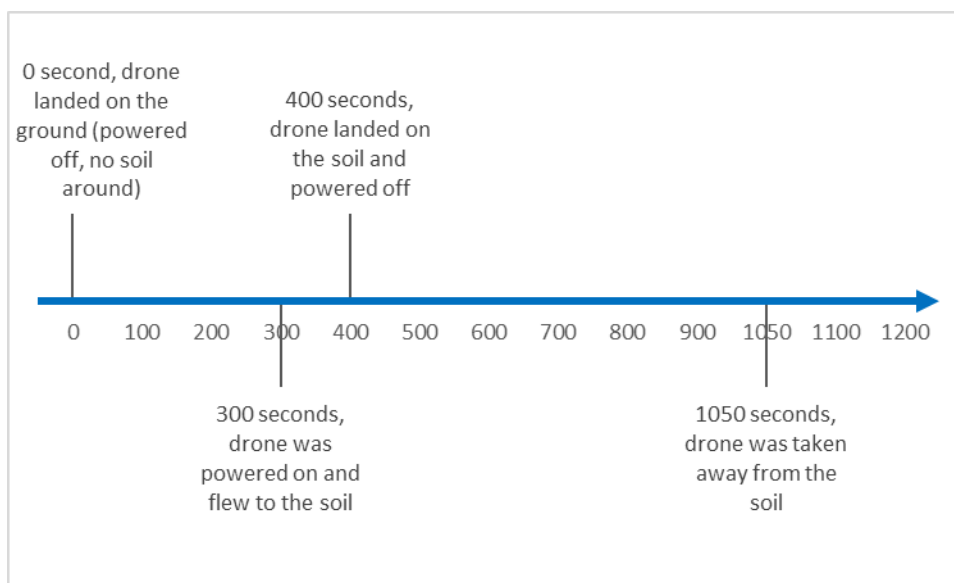
All the tests started at 150s and ended at 800s.



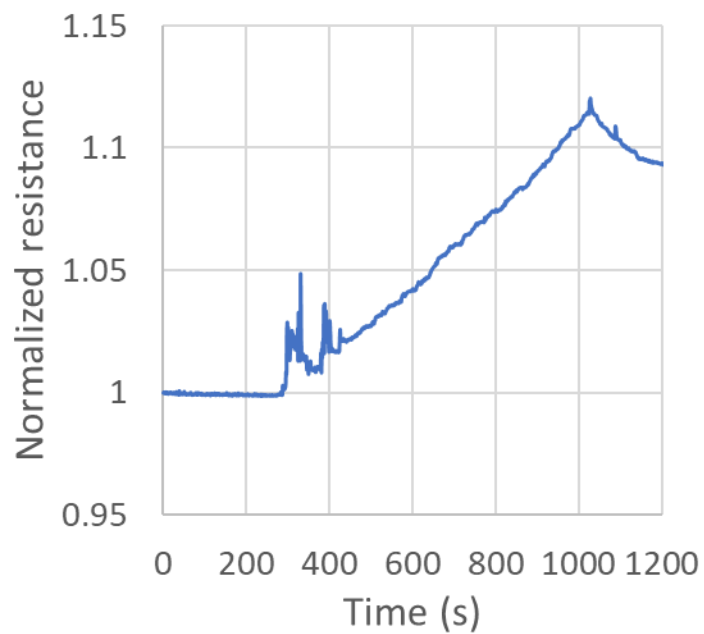
Figure 11: soil-sand mixture in the Pyrex® 150x75 mm crystallizing dish.

3.5 DRONE TEST RESULT AND DISCUSSION

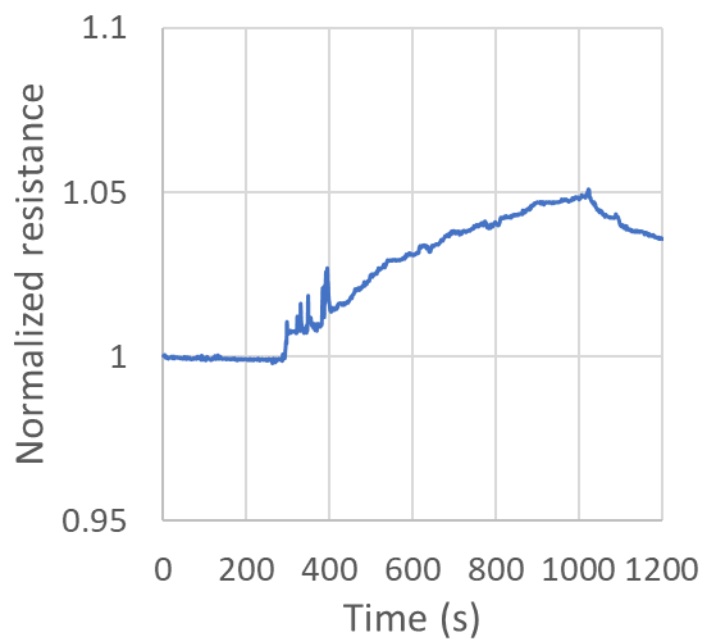
Figure 11 gives the drone test result. The drone was at still from 0 to 300 seconds. It was powered up and flew to the soil from 300 seconds to 400 seconds. Then it landed on the soil and powered off from 400 to 1050 seconds. The timeline is shown in figure 11(a). From the test result, it shows that the airflow generated by the drone had non-neglectable influence on the sensors. The pure SWCNT sensor had a resistance change of around 10-12%, the Nafion-coated SWCNT sensor had a resistance change of around 3-5%, and the PEI-coated SWCNT sensor had a resistance change of around 34% with a lot of large fluctuations during the test.



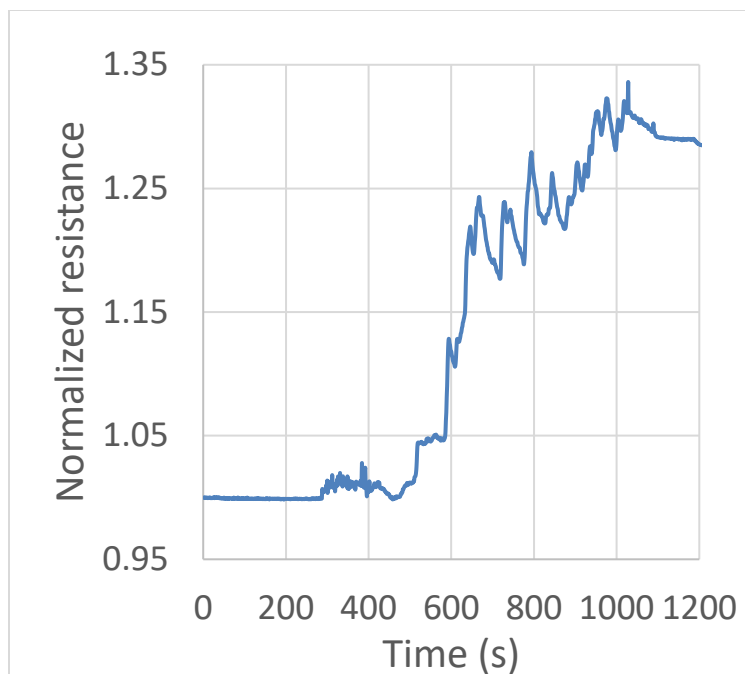
(a)



(b)



(c)



(d)

Figure 12: Drone test result. (a) Drone test timeline. (b) Pure SWCNT resistance change. (c) Nafion-coated SWCNT resistance change. (d) PEI-coated SWCNT resistance change.

Based on pure SWCNT and Nafion-coated SWCNT calibration curves, the ammonia concentration of this pot of fertilized soil was around 3-5 ppm. The PEI-coated SWCNT showed a large resistance increase. Such large increase was not shown neither in the ammonia test nor in the soil test. This result may be caused by two factors. The first one is that the ammonia test and the soil test were done in a sealed chamber, but the drone test was done in open air. There were possible more influences that PEI-coated SWCNT sensor was sensitive to in the open air. For example, with sufficient oxygen supplied, some chemical reactions may be more active. The second one is that the amount of soil. The in-chamber soil test used 30g of fertilized soil, but the drone test used much more amount of soil. The major gases in the 30g of soil may be ammonia

and NO_x . For large amount of soil, due to the microbe activity, gases other than ammonia and NO_x may become major.

3.6 SUMMERY

Using single walled carbon nanotube (SWCNT) sensors, ammonia and NO_x gases were detected in sand mixed with fertilizer. The developed sensor array was integrated into a drone for gas detection in soil. In the experiment, the combination of pure SWCNT sensor, Nafion-coated SWCNT sensor and PEI-coated SWCNT sensor had a relatively accurate characteristic curve in the ammonia concentration range of 1 ~ 50 ppm. When the concentration range decreased to 10ppb to 1ppm, the characteristic curve was not highly accurate, but still could provide a concentration range.

Regarding the recovery time of the SWCNT sensors, the larger resistance change required the longer recovery time. For example, when tested with 50ppm of ammonia, the recovery time was over 24 hours. As for the low concentration, the recovery time was much shorter. The sensors required about 10 minutes to recovery after the 10ppb ammonia test.

As for the soil test, it was found that this sensor set was able to provide a reference value of the ammonia concentration in soil. According to the soil test, the minimum concentration that the sensors had response was around 50 ppb. When mixed with sand, the detection limit of the SWCNT sensor was 1:100 of the minimum soil-sand ratio. Even though the PEI-coated SWCNT sensor's responses might not only because of ammonia as discussed earlier, a possible maximum ammonia concentration could still be estimated by comparing the results of pure SWCNT sensor and Nafion-coated SWCNT sensor with their calibration curves. Since this set of sensors would be used as a low-cost ammonia monitor for agriculture, this accuracy should be good enough to detect the ratio of fertilizer to sand.

To further improve the performance of these sensors, more experiment needs to be done to determine the influential factors for a PEI-coated SWCNT sensor. The design of the 3D-printed case for the drone test needs to be improved to reduce the effect of the airflow generated by the drone.

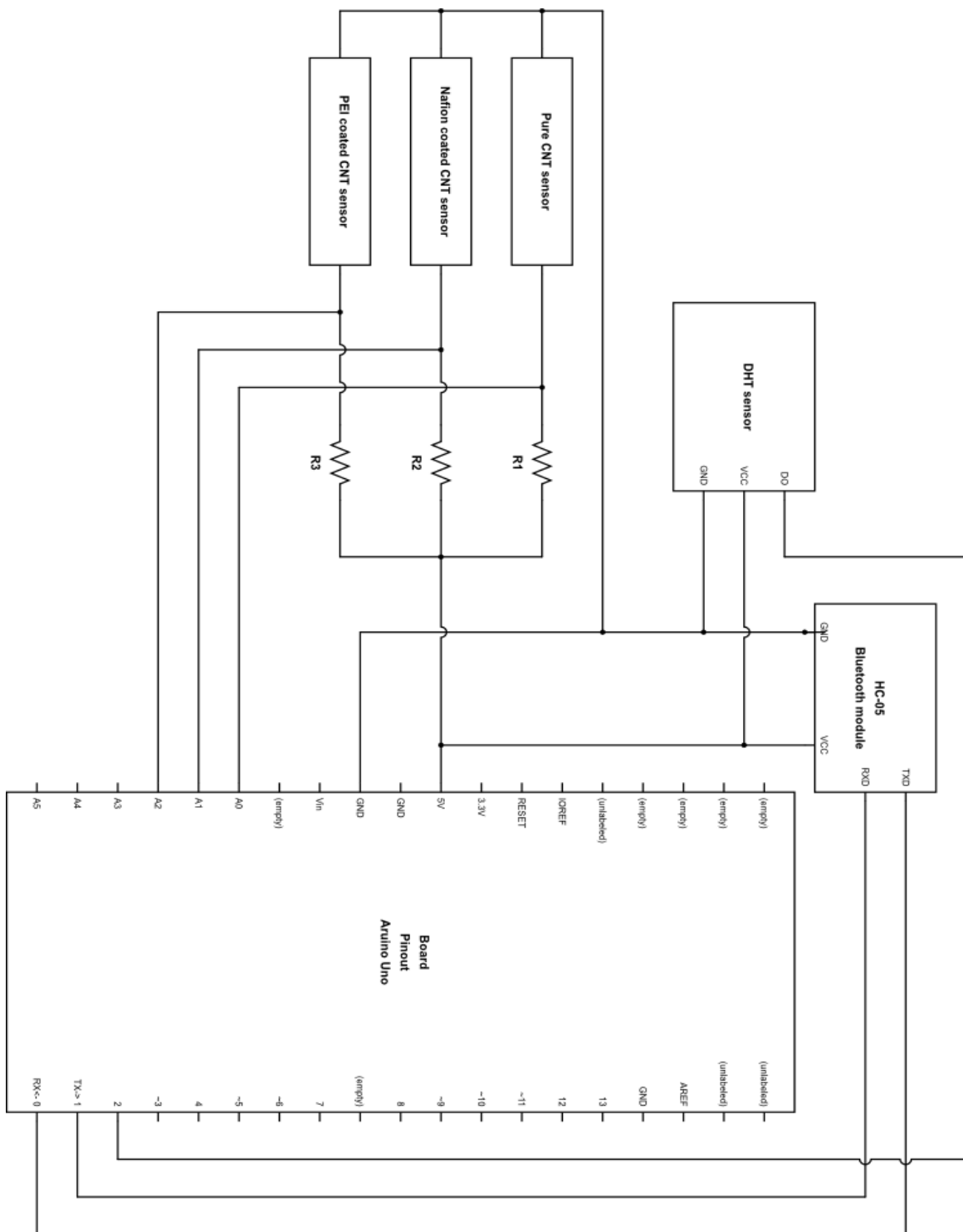
REFERENCES

- [1] U. Diaz, V. Saliba-Colombani, O. Loudet, P. Belluomo, L. Moreau, F. Daniel-Vedele, *et al.*, "Leaf yellowing and anthocyanin accumulation are two genetically independent strategies in response to nitrogen limitation in *Arabidopsis thaliana*," *Plant and Cell Physiology*, vol. 47, pp. 74-83, Jan 2006.
- [2] T. Kraiser, D. E. Gras, A. G. Gutierrez, B. Gonzalez, and R. A. Gutierrez, "A holistic view of nitrogen acquisition in plants," *Journal of Experimental Botany*, vol. 62, pp. 1455-1466, Feb 2011.
- [3] C. W. Liu, Y. Sung, B. C. Chen, and H. Y. Lai, "Effects of Nitrogen Fertilizers on the Growth and Nitrate Content of Lettuce (*Lactuca sativa* L.)," *International Journal of Environmental Research and Public Health*, vol. 11, pp. 4427-4440, Apr 2014.
- [4] G. P. Robertson and P. M. Vitousek, "Nitrogen in Agriculture: Balancing the Cost of an Essential Resource," in *Annual Review of Environment and Resources*. vol. 34, ed Palo Alto: Annual Reviews, 2009, pp. 97-125.
- [5] I. Cechin and T. D. Fumis, "Effect of nitrogen supply on growth and photosynthesis of sunflower plants grown in the greenhouse," *Plant Science*, vol. 166, pp. 1379-1385, May 2004.
- [6] D. L. Zhao, K. R. Reddy, V. G. Kakani, J. J. Read, and G. A. Carter, "Corn (*Zea mays* L.) growth, leaf pigment concentration, photosynthesis and leaf hyperspectral reflectance properties as affected by nitrogen supply," *Plant and Soil*, vol. 257, pp. 205-217, Nov 2003.
- [7] N. Anderson, R. Strader, and C. Davidson, "Airborne reduced nitrogen: ammonia emissions from agriculture and other sources," *Environment International*, vol. 29, pp. 277-286, Jun 2003.
- [8] R. Conrad, W. Seiler, and G. Bunse, "FACTORS INFLUENCING THE LOSS OF FERTILIZER NITROGEN INTO THE ATMOSPHERE AS N₂O," *Journal of Geophysical Research-Oceans*, vol. 88, pp. 6709-6718, 1983.
- [9] O. E. Sala, F. S. Chapin, J. J. Armesto, E. Berlow, J. Bloomfield, R. Dirzo, *et al.*, "Biodiversity - Global biodiversity scenarios for the year 2100," *Science*, vol. 287, pp. 1770-1774, Mar 2000.
- [10] L. Jones, A. Provins, M. Holland, G. Mills, F. Hayes, B. Emmett, *et al.*, "A review and application of the evidence for nitrogen impacts on ecosystem services," *Ecosystem Services*, vol. 7, pp. 76-88, Mar 2014.
- [11] S. M. McGinn and H. H. Janzen, "Ammonia sources in agriculture and their measurement," *Canadian Journal of Soil Science*, vol. 78, pp. 139-148, Feb 1998.
- [12] J. N. Galloway, F. J. Dentener, D. G. Capone, E. W. Boyer, R. W. Howarth, S. P. Seitzinger, *et al.*, "Nitrogen cycles: past, present, and future," *Biogeochemistry*, vol. 70, pp. 153-226, Sep 2004.
- [13] X. Zhu, W. Zhang, H. Chen, and J. Mo, "Impacts of nitrogen deposition on soil nitrogen cycle in forest ecosystems: A review," *Acta Ecologica Sinica*, vol. 35, pp. 35-43, 2015/06/01/ 2015.
- [14] N. B. Dise, M. Ashmore, S. Belyazid, A. Bleeker, R. Bobbink, W. de Vries, *et al.*, "Nitrogen as a threat to European terrestrial biodiversity," in *The European Nitrogen Assessment: Sources, Effects and Policy Perspectives*, A. Bleeker, B. Grizzetti, C. M.

- Howard, G. Billen, H. van Grinsven, J. W. Erisman, *et al.*, Eds., ed Cambridge: Cambridge University Press, 2011, pp. 463-494.
- [15] J. A. Silva, R. S. Uchida, U. o. H. a. M. C. o. T. Agriculture, and H. Resources, *Plant Nutrient Management in Hawaii's Soils: Approaches for Tropical and Subtropical Agriculture*: College of Tropical Agriculture & Human Resources, University of Hawaii at Manoa, 2000.
- [16] K. W. T. Goulding, "Soil acidification and the importance of liming agricultural soils with particular reference to the United Kingdom," *Soil Use and Management*, vol. 32, pp. 390-399, Sep 2016.
- [17] L. Xiankai, M. Jiangming, and D. Shaofeng, "Effects of nitrogen deposition on forest biodiversity," *Acta Ecologica Sinica*, vol. 28, pp. 5532-5548, 2008/11/01/ 2008.
- [18] N. Vanbreemen, C. T. Driscoll, and J. Mulder, "ACIDIC DEPOSITION AND INTERNAL PROTON SOURCES IN ACIDIFICATION OF SOILS AND WATERS," *Nature*, vol. 307, pp. 599-604, 1984.
- [19] T. Dirnbock, G. Proll, K. Austnes, J. Beloica, B. Beudert, R. Canullo, *et al.*, "Currently legislated decreases in nitrogen deposition will yield only limited plant species recovery in European forests," *Environmental Research Letters*, vol. 13, Dec 2018.
- [20] J. N. Galloway, A. R. Townsend, J. W. Erisman, M. Bekunda, Z. C. Cai, J. R. Freney, *et al.*, "Transformation of the nitrogen cycle: Recent trends, questions, and potential solutions," *Science*, vol. 320, pp. 889-892, May 2008.
- [21] W. Q. AL-Bukhaiti, A. Noman, A. S. Qasim, and A. Al-Farga, "Gas Chromatography : Principles , Advantages and Applications in Food Analysis," 2017.
- [22] A. Bertrand, "BRANDY AND COGNAC | Armagnac, Brandy, and Cognac and their Manufacture," in *Encyclopedia of Food Sciences and Nutrition (Second Edition)*, B. Caballero, Ed., ed Oxford: Academic Press, 2003, pp. 584-601.
- [23] B. Boggess, "Mass Spectrometry Desk Reference (Sparkman, O. David)," *Journal of Chemical Education*, vol. 78, p. 168, 2001/02/01 2001.
- [24] J. B. Nowak, J. A. Neuman, K. Kozai, L. G. Huey, D. J. Tanner, J. S. Holloway, *et al.*, "A chemical ionization mass spectrometry technique for airborne measurements of ammonia," *Journal of Geophysical Research-Atmospheres*, vol. 112, Feb 2007.
- [25] L. Clarisse, C. Clerbaux, F. Dentener, D. Hurtmans, and P. F. Coheur, "Global ammonia distribution derived from infrared satellite observations," *Nature Geoscience*, vol. 2, pp. 479-483, Jul 2009.
- [26] L. B. Mendes, N. W. M. Ogink, N. Edouard, H. J. C. van Dooren, I. D. F. Tinoco, and J. Mosquera, "NDIR Gas Sensor for Spatial Monitoring of Carbon Dioxide Concentrations in Naturally Ventilated Livestock Buildings," *Sensors*, vol. 15, pp. 11239-11257, May 2015.
- [27] X. Liu, S. T. Cheng, H. Liu, S. Hu, D. Q. Zhang, and H. S. Ning, "A Survey on Gas Sensing Technology," *Sensors*, vol. 12, pp. 9635-9665, Jul 2012.
- [28] B. Timmer, W. Olthuis, and A. van den Berg, "Ammonia sensors and their applications - a review," *Sensors and Actuators B-Chemical*, vol. 107, pp. 666-677, Jun 2005.
- [29] B. D. Hale, B. Fairchild, J. Worley, L. Harper, C. Ritz, M. Czarick, *et al.*, "Comparison of ammonia measurement methods inside and outside tunnel-ventilated broiler houses," *Journal of Applied Poultry Research*, vol. 19, pp. 245-262, Sep 2010.
- [30] K. G. Ong, K. F. Zeng, and C. A. Grimes, "A Wireless, Passive Carbon Nanotube-Based Gas Sensor," *Ieee Sensors Journal*, vol. 2, pp. 82-88, Apr 2002.

- [31] J. W. Han, B. Kim, J. Li, and M. Meyyappan, "A carbon nanotube based ammonia sensor on cotton textile," *Applied Physics Letters*, vol. 102, May 2013.
- [32] F. Goudarzi, M. R. Vaezi, and A. Kazemzadeh, "A novel single wall carbon nanotubes-based sensor doped with lithium for ammonia gas detection," *Journal of Ceramic Processing Research*, vol. 13, pp. 612-616, Oct 2012.
- [33] S. J. Young and Z. D. Lin, "Ammonia gas sensors with Au-decorated carbon nanotubes," *Microsystem Technologies-Micro-and Nanosystems-Information Storage and Processing Systems*, vol. 24, pp. 4207-4210, Oct 2018.
- [34] L. K. Randeniya, P. J. Martin, A. Bendavid, and J. McDonnell, "Ammonia sensing characteristics of carbon-nanotube yarns decorated with nanocrystalline gold," *Carbon*, vol. 49, pp. 5265-5270, Dec 2011.
- [35] M. Chiesa, F. Rigoni, M. Paderno, P. Borghetti, G. Gagliotti, M. Bertoni, *et al.*, "Development of low-cost ammonia gas sensors and data analysis algorithms to implement a monitoring grid of urban environmental pollutants," *Journal of Environmental Monitoring*, vol. 14, pp. 1565-1575, Jun 2012.
- [36] H. Z. Geng, K. K. Kim, C. Song, N. T. Xuyen, S. M. Kim, K. A. Park, *et al.*, "Doping and de-doping of carbon nanotube transparent conducting films by dispersant and chemical treatment," *Journal of Materials Chemistry*, vol. 18, pp. 1261-1266, 2008.
- [37] S. L. Kim, K. Choi, A. Tazebay, and C. Yu, "Flexible Power Fabrics Made of Carbon Nanotubes for Harvesting Thermoelectricity," *Acs Nano*, vol. 8, pp. 2377-2386, Mar 2014.

APPENDIX A



APPENDIX B

Arduino code for MQ-135 calibration:

```
#include "MQ135.h"
#include <DHT.h>
#define DHTPIN 2 // modify to the pin we connected
#define DHTTYPE DHT21 // DHT 21 (AM2301)
DHT dht(DHTPIN, DHTTYPE);
#define PIN_MQ135 A2
MQ135 mq135_sensor = MQ135(PIN_MQ135);

void setup() {
  Serial.begin(9600);
}

void loop() {
  //read humidity and temperature form the h&t sensor
  float humidity = dht.readHumidity();
  float temperature = dht.readTemperature();

  //get the MQ135 sensor resistance
  float resistance = mq135_sensor.getResistance();

  //get the correction factor
  float CorrectionFactor = mq135_sensor.getCorrectionFactor(temperature, humidity);

  //get the corrected resistance
  float CorrectedResistance = mq135_sensor.getCorrectedResistance(temperature, humidity);
```

```
//print out the results
Serial.print("\t temperature: ");
Serial.print(temperature);
Serial.print("\t humidity: ");
Serial.print(humidity);
Serial.print("\t CorrectedResistance: ");
Serial.print(CorrectedResistance,5);
Serial.println();

delay(1000)
}
```

